World Academy of Science, Engineering and Technology
International Journal of Materials and Metallurgical Engineering
Vol:12, No:1, 2018

Effect of Retained Austenite Stability in Corrosion Mechanism of Dual Phase High Carbon Steel

W. Handoko, F. Pahlevani, V. Sahajwalla

***Abstract*—**Dual-phase high carbon steels (DHCS) are commonly known for their improved strength, hardness, and abrasive resistance properties due to co-presence of retained austenite and martensite at the same time. Retained austenite is a meta-stable phase at room temperature, and stability of this phase governs the response of DHCS at different conditions. This research paper studies the effect of RA stability on corrosion behaviour of high carbon steels after they have been immersed into 1.0 M NaCl solution for various times. For this purpose, two different steels with different RA stabilities have been investigated. The surface morphology of the samples before and after corrosion attack was observed by secondary electron microscopy (SEM) and atomic force microscopy (AFM), along with the weight loss and Vickers hardness analysis. Microstructural investigations proved the preferential attack to retained austenite phase during corrosion. Hence, increase in the stability of retained austenite in dual-phase steels led to decreasing the weight loss rate.

***Keywords*—**High carbon steel, austenite stability, atomic force microscopy, corrosion.

I. Introduction

IN recent decades, the utilisation of DHCS has been vastly increased in various industrial applications, due to its superior properties in strength, hardness, toughness, high wear and abrasive resistance [1]. This DHCS steel contains retained austenite (RA) and martensite microstructures that are capable to withstand the high wear and shear conditions. In addition to its distinctive properties, the extensive knowledge about RA stability by adding different chromium content towards the corrosion mechanism is essential for assessing the potential of this steel in different application. Ma et al. [2], Kadhum et al. [3], and Shuaib-Babata and Abdulqadir [4] have researched the influence of a different single-phase microstructure on corrosion behaviour of mild steels, but limited investigation has been carried out on DHCSs. It is imperative to understand the characterization of this steel corrosion in sodium chloride solution, in order to establish applications with cost-effective alternative.

Chromium is commonly supplemented as one of the important alloying elements in steel to improve its hardenability and corrosion resistance properties and to prevent oxidation [5]-[7]. However, to achieve the economical high carbon steel parts with excellent properties, which can be used in many manufacturing applications, it is essential to understand function of chromium and its influence on the microstructure of dual-phase steels.

The objective of the current study is to address the relevant knowledge gap in order to assess the influence of stable RA towards the corrosion mechanism of DHCS in 1.0 M NaCl solution. The investigation was based on two different RA volume fractions with chromium percentage. This investigation provides an opportunity to enhance its corrosion-resistant property and to minimize the reliability on alloying elements and compositional modification of DHCS products for cost reduction.

II. Experimental

A. Materials

Two different high carbon steels with different Cr contents, which result in different RA percentages, have been used in this study. Sample A contains 0.10%-0.20% Cr with 46-51% RA, and Sample B contains 1.90%-2.20% Cr with 56%-60% RA.

B. Sample Preparation

All samples were cut to suit all the instrument's requirements (4 mm x 4 mm x 3 mm), grinded with silicon carbide abrasive paper to 4000 grit and polished in sequence up to 1 μm with diamond suspension, then they were rinse with ethanol, cleaned by using ultrasonic cleaner and dried. The samples were immersed into the corrosive solution of 1.0 M NaCl up to two hours. Weight loss analysis was conducted to compare the original weight and final weight loss after corrosion attack. The precision laboratory scale, Sartorius CP124S was used to measure the accurate values of weight loss.

C. Microstructural Investigation

The microstructures of the steel samples have been investigated using optical microscopy Nikon Eclipse ME-600.

SEM analysis has been performed with Hitachi S-3400I to analyze the surface morphology of the dual-phase steel in high resolution (accelerating voltage at 15 keV).

D. Atomic Force Microscopy

Effect of corrosion on the surface roughness of steel was carried out by AFM with Bruker BioScope Catalyst.

The area of 5 μm x 5 μm was constantly scanned to acquire consistent result before and after corrosion attack. Evolution of the surface roughness for martensite-austenite phases from the beginning until a designated time (2 hours) was visibly

Wilson Handoko is PhD Candidate and Research Assistant with UNSW Sydney, NSW 2052, Australia (phone: (+61) 425-958-088; e-mail: w.handoko@unsw.edu.au).

Farshid Pahlevani is Senior Research Fellow in SMaRT centre at UNSW Sydney, NSW 2052, Australia (e-mail: f.pahlevani@unsw.edu.au).

Veena Sahajwalla is director of SMaRT Centre and Laureate Professor in UNSW Sydney, NSW 2052, Australia (e-mail: veena@unsw.edu.au).

observed by using this technique from AFM analysis.

E. Vickers Hardness Tests

The hardness of samples before and after corrosion was measured by Struers DuraScan instrument that was equipped with Vickers pyramidal diamond indenter. The hardness test was carried out with HV10 mode for four times on different location of the sample to obtain average hardness of each condition.

III. Results and Discussion

A. Morphology

At microscale analysis by optical microscopy, comparison results of Figs. 1 and 2 present the volume fraction of RA and martensite phases of sample A and B after etching process with 2% nital etchant or before immersion into 1.0 M NaCl media. It is visible that dual-phase steel with lower chromium percentage has lower RA volume fraction (white colour region) than the steel with higher chromium percentage. The less stable RA possesses lengthy and bulky martensite grain size with fine RA, whereas improved RA stability has skinny and less packed of martensitic microstructure with larger block of RA phase. In addition, from this result, it can be observed that for different chemical composition on dual-phase steel, different chromium content can define the percentage of martensite and its stability of RA in dual-phase steel and it can offer contrastive corrosion resistance properties.

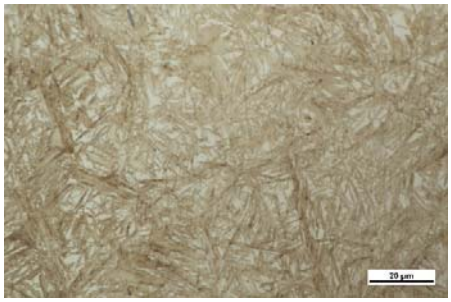

Fig. 1 Optical microscopy of sample A at magnification of 100x – etched or before immersion into 1.0 M NaCl solution

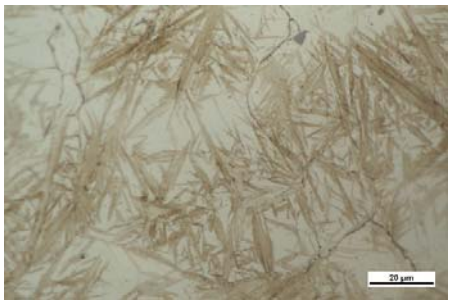

Fig. 2 Optical microscopy of sample B at magnification of 100x – etched or before immersion into 1.0M NaCl solution

After optical microscope analysis, further investigation was conducted with SEM analysis up to ~5,000x magnification to perform this preferential damage on austenite phase at the initial stage. Fig. 3 indicates the etched surface of DHCS - sample A (with 46%-51% RA) before the immersion into corrosive media. The grain boundary corrosion between austenite and martensite interfaces is visible, including visible polishing scratches. After one hour of corrosion attack, it performed preferential attack on RA as very significant damage occurred on this phase. Moreover, pit holes started to form as the austenitic structure collapsed with little degradation on martensitic structure after two hours of immersion as present in Fig. 4.

On the other hand, in Fig. 5, the visible austenite-martensite microstructures and insignificant grain boundary corrosion between dual-structure interfaces can also be observed on sample B after etching process. Fig. 6 presents the sample B (with 56%-60% RA) after corrosion for two hours that had non-vital surface modification on austenite microstructure, but moderate damage on martensite phase exists, as this specimen possessed lower martensitic percentage, yet higher austenite volume fraction than sample A in which it led to better austenitic stability on propensity to corrosion attack, improved in corrosion-resistant property. The corrosion resistance properties on sample B were superior than sample A, as the influence of its higher volume percentage of austenite phase in DHCS that led to metastable RA microstructures with reduced in martensitic phase [8], [9]; thus, sample B is able to resist more towards the corrosion attack. Furthermore, it can be predicted that the corrosion mechanism in this DHCS is localised form of corrosion as it generated cavities from outer to inner surface of the steels or it is well known as pitting corrosion. The main reason of this occurrence can be due to the varied boundary shapes on both microstructures that connect martenite-austenite interfaces and stabilities of different austenitic phase, further investigation in nano-resolution is described in the AFM results section. The microstructural results will be corresponded to the weight loss measurement in which higher metastable RA had lower susceptibility to corrosion damage, hence decreased in weight loss as it had lower corrosion rate compared with low RA percentage with lower stability.

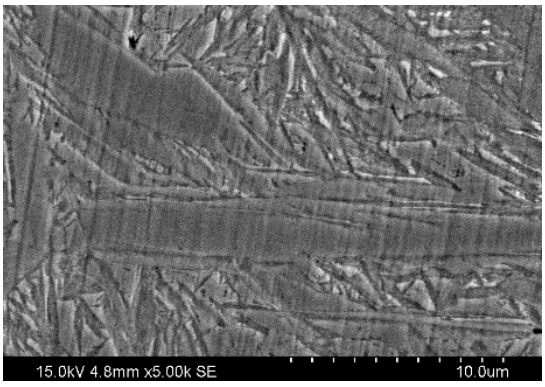

Fig. 3 SEM imaging of sample A at magnification of 5.000x in etched condition

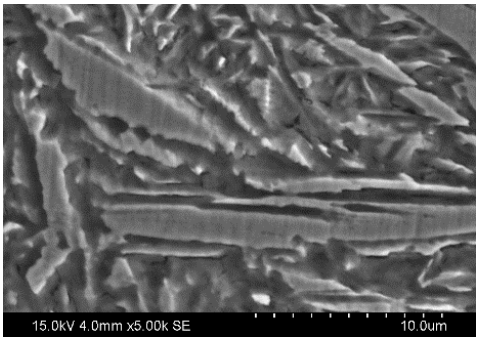

Fig. 4 SEM imaging of sample A at magnification of 5,000x after 2h immersion into 1.0M NaCl solution

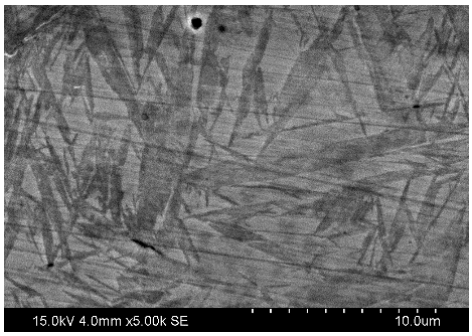

Fig. 5 SEM imaging of sample B at magnification of 5.000x in etched condition

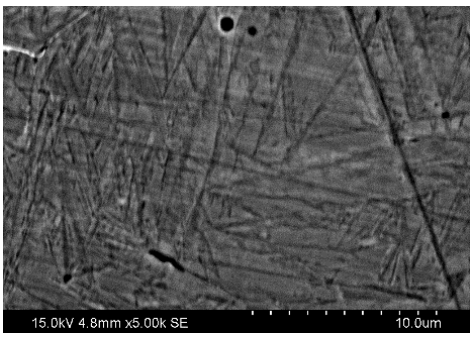

Fig. 6 SEM imaging of sample B at magnification of 5,000x after 2h immersion into 1.0M NaCl solution

B. Corrosion Mechanism

The weight loss measurement was conducted, in order to determine the slowing corrosion rate, as the more stable RA phase has less internal energy and it is able to resist corrosion attack in the corrosive solution. Table I represents the reduction in corrosion rate between first and second hours of the immersion in corrosive media. On sample A, a massive weight loss accounted to 8.990% after two hours of corrosion, as it possessed the higher level of RA stability, while sample B made contribution of 0.211% weight loss. All samples showed similar behaviour in which the weight loss was significantly higher in first hour than second hour, this is because of both microstructures corroded at different rate and difference in internal energy between martensite-austenite interfaces. From this weight loss analysis, the improved stability of RA microstructure resists more towards the corrosion damage; hence, it leads to decrease in corrosion rate.

TABLE I
A COMPARISON OF WEIGHT LOSS AFTER CORROSION ATTACK AT 0H, 1H AND 2 HOURS ON DHCS

Time (h)	Weight Loss (%)	
	Sample A	Sample B
0	0.000	0.000
1	5.688	0.175
2	8.990	0.211

The nanoscale topography imaging was conducted with AFM to perform real time evolution of DHCS in the corrosive media. This AFM has been employed in some corrosion studies with broad range of materials in different corrosive solution [10] that can offer a very fine resolution of topographical information [11], [12]. The AFM results were analysed, in which Fig. 7 presents the sample A before immersion into NaCl solution, as polished scratches were clearly visible on the surface of the sample. It was found that a unique phenomenon occurred after half an hour into corrosion attack, in which significant changes on surface was occurred.

Fig. 8 demonstrates the surface evolution of the sample A before corrosion attack. Obvious rough surface, which was produced at this point, suggested that another evidence of preferential attack on one phase – austenite was then followed by the martensite. Fig. 9 represented the sample B without etching, similarly the scratches were observable in nanoscale image scanning. It remained unchanged until the first hour of experiment and similar corrosion behaviour occurred after that as such in Fig. 10, since this steel sample possessed more stable austenitic phase as it leads to less martensitic volume fraction on dual-phase steel, thus improving the corrosion resistant properties.

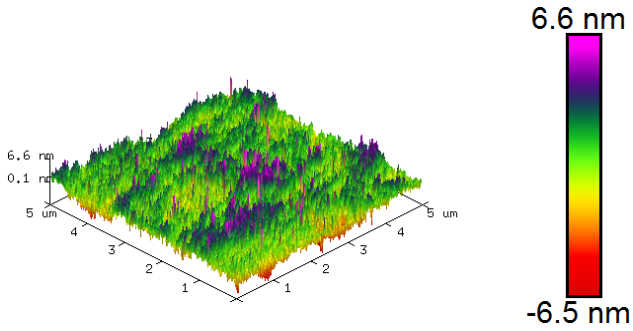

Fig. 7 AFM topographical imaging of sample A in the air condition without etching or before immersion into 1.0 M NaCl solution

The effect of RA microstructure stability in corrosion mechanism can be observed in the nanoscale level, where austenite phase began to degrade in sample A as it possessed lower RA percentage than sample B, hence austenitic structure is more susceptible to corrosion attack with dependency on its stability. Austenitic phase was propensity to corrosive solution, due to large grain size shape on austenite and lower martensite distribution on DHCS in which minimized its grain boundary density, hence decreased on grain boundary

corrosion rate [13].

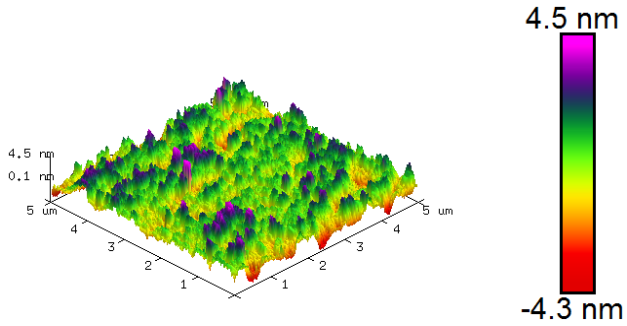

Fig. 8 AFM topographical imaging of sample A after 2 hours of immersion into 1.0 M NaCl solution

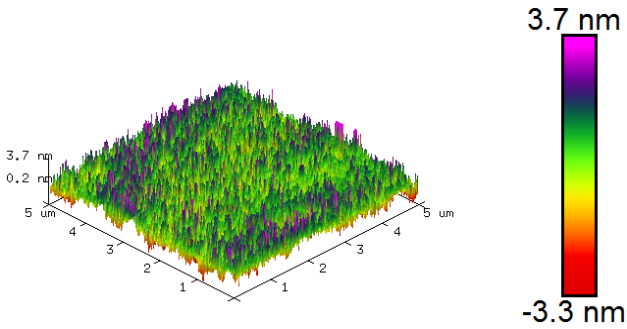

Fig. 9 AFM topographical imaging of sample B in the air condition without etching or before immersion into 1.0M NaCl solution

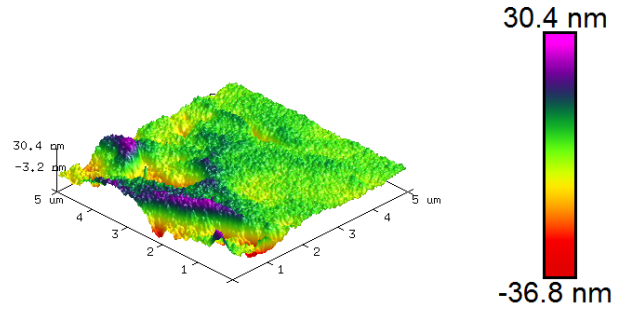

Fig. 10 AFM topographical imaging of sample B after 2 hours of immersion into 1.0 M NaCl solution

C. Hardness Properties

The DHCS specimens were undergone Vickers hardness test to assess the effect of different RA stability on hardness property as shown in Table II. Sample A performed a substantial loss of hardness properties, proximately three times higher (from 7.326 GPa to 7.289 GPa) than sample B at 0.505% in correlated results with the weight loss analysis. On the other hand, sample B made a contribution of approximately 0.166% reduction of hardness property. Moreover, insignificant decreased hardness value on sample B was due to higher volume fraction of RA than sample A, this prevented pitting holes to be generated more between the grain boundary interfaces, thus improved the austenitic stability and reduced the susceptibility towards corrosion attack. Although some alloying elements including chromium have a major role in enhancement of hardness properties on steel [14]-[16], the loss of austenite and martensite phases by corrosion damage has the influence on its hardness properties. This means that increase in volume fraction of RA improved its stability as well as led to reduction in internal energy between each phase and enhanced hardness property towards corrosive solution. As the results, from this corrosion test on DHCS samples, it can be concluded that overall corrosion mechanism is pitting corrosion, as pit holes were aroused on the outer surface of both austenite and martensite microstructures.

TABLE II
COMPARISON OF HARDNESS ON HIGH CARBON STEEL SAMPLES BEFORE AND AFTER IMMERSION INTO CORROSIVE SOLUTION AT 0H, 1H AND 2H

Time (h)	Hardness (GPa)	
	Sample A	Sample B
0	7.326	7.846
1	7.306	7.838
2	7.289	7.833

IV. CONCLUSION

This research has shown that the corrosion rates varied marginally between two different DHCS samples. Microstructural, mechanical and corrosion resistant analyses were carried out for DHCS specimens to examine the preferential attack on one phase then followed by another. As the volume percentage of RA increased, it promoted improvement of its stability, minimized the internal energy between martensite-austenite grain boundary interfaces and lowered the propensity on corrosion attack, thus decreased the corrosion rate. The bulky austenite grain structure with less distribution of martensite grain offers better corrosion resistance properties, due to the decrease in grain boundary density in which less surface area contacted between each interface that led to reduction of grain boundary corrosion. This finding is crucial to produce DHCS products with excellent properties that offer opportunities to acknowledge and predict corrosion characterization, and optimization of corrosion-resistant properties with minimization to reliance on alloying elements for cost-effective in many manufacturing applications.

ACKNOWLEDGMENT

This research was supported under Australian Research Council's Industrial Transformation Research Hub funding scheme (project IH130200025). We gratefully acknowledge the technical support provided by the Analytical Centre in the UNSW Australia.

REFERENCES

[1] A. Calik, A. Duzgun, O. Sahin and N. Ucar. Effect of Carbon Content on the Mechanical Properties of Medium Carbon Steels. Zeitschrift für Naturforschung A, 65(5), 2010, pp. 468-472.
[2] Y. Ma, Y. Li and F. Wang. Corrosion of low carbon steel in atmospheric environments of different chloride content. *Corrosion Science*, 51(5), 2009, pp.997-1006.
[3] A. Kadhum, A. Mohamad, L. Hammed, A. Al-Amiery, N. San and A. Musa. Inhibition of Mild Steel Corrosion in Hydrochloric Acid Solution by New Coumarin. *Materials*, 7(6), 2014, pp.4335-4348.

[4] Y. L. Shuaib-Babata and B. L. Abdulqadir. Corrosion Behaviours of Commercial Low Carbon Steel in Petroleum Environment. SEEM Journal Research & Development, 1(1), 2012, pp. 18-29.
[5] J. Davis. *Properties and Selection: Irons, Steels and High-Performance Alloys*. Materials Park, OH: ASM International, 2007.
[6] M. Fong-Yuan. Corrosive Effects of Chlorides on Metals, Pitting Corrosion, Prof. Nasr Bensalah (Ed.). INTECH Open Access Publisher, 2012.
[7] C. Chen, M. Lu, D. Sun, Z. Zhang and W. Chang. Effect of Chromium on the Pitting Resistance of Oil Tube Steel in a Carbon Dioxide Corrosion System. *CORROSION*, 61(6), 2005, pp.594-601.
[8] R. Hossain, F. Pahlevani, M. Quadir and V. Sahajwalla. Stability of retained austenite in high carbon steel under compressive stress: an investigation from macro to nano scale. Scientific Reports, 6(1), 2016.
[9] ASTM International. Chapter 6: Austenitic Stainless Steel. Stainless Steels for Design Engineers, 2008, pp. 69-78.
[10] O. Olivares-Xometl, N.V. Likhanova, M.A. Dominguez-Aguilar, J.M. Hallen, L.S. Zamudio, E. Arce, Surface analysis of inhibitor films formed by imidazolines and amides on mild steel in an acidic environment, Applied Surface Science 252 (6), 2006, pp. 2139–2152.
[11] L. Xu, K. Chan, H.H.P. Fang, Application of atomic force microscopy in the study of microbiologically influenced corrosion, *Materials Characterization.* 48 (2–3), 2002, pp. 195–203.
[12] R. Wang, An AFM and XPS study of corrosion caused by micro-liquid of dilute sulfuric acid on stainless steel, *Applied Surface Science*. 227 (1–4), 2004, pp. 399– 409.
[13] T. Remmerswaal. "The influence of microstructure on the corrosion behaviour of ferritic-martensitic steel: 3.2 Influence of prior austenite grain size on corrosion properties". Delft University of Technology, 2015, pp. 57-62.
[14] S. Trivedi, Y. Mehta, K. Chandra and P. S. Mishra. Effect of Chromium on Mechanical Properties of Powder-Processed Fe-0.35wt% P Alloys. Journal of Minerals & Materials Characterization & Engineering, 8 (8), 2009, pp. 611-620.
[15] N. Poolthong, H. Nomura and M. Takita. Effect of Heat Treatment on Microstructure and Properties of Semi-solid Chromium Cast Iron. *Materials Transactions*, 45(3), 2004, pp.880-887.
[16] H. Jirková, L. Kučerová and B. Mašek. The Effect of Chromium on Microstructure Development during Q-P Process. *Materials Today*: *Proceedings*, 2, 2015, pp.S627-S630.